

Cooperative response of $\text{Pb}(\text{ZrTi})\text{O}_3$ nanoparticles to curled electric fields

Ivan I. Naumov and Huaxiang Fu

Department of Physics, University of Arkansas, Fayetteville, AR 72701, USA

(Dated: November 6, 2018)

Abstract

Using first-principles based effective Hamiltonian and finite temperature Monte Carlo simulations we investigate cooperative responses, as well as microscopic mechanism for vortex switching, in zero-dimensional $\text{Pb}(\text{Zr}_{0.5}\text{Ti}_{0.5})\text{O}_3$ nanoparticles under curled electric fields. We find that the generally accepted domain coexistence mechanism is not valid for toroid switching. Instead dipoles are shown to display unusual collective behaviors by forming a new vortex with perpendicular (but not opposite) toroid moment. The strong correlation between the new and original vortices is revealed to be critical for reversing toroid moment. Microscopic insight for the puzzling collective response is discussed. Based on our finding, we further describe a technological approach that is able to drastically reduce the magnitude of the curled electric field needed for vortex switching.

In the study of ferroelectric physics, one field that is currently attracting widespread attention is low-dimensional ferroelectrics (FEs).[1, 2, 3, 4, 5] Among FE nanostructures that have been synthesized, FE nanoparticles are particularly interesting because the strong depolarizing fields along all three directions force dipoles in these particles to adopt a topological vortex configuration,[6] which is a new form of dipole ordering[7]. This ordering opens up a different class of cooperative phenomena and phase transitions in FEs of reduced dimension, which is a subject that has generated long-standing interest for decades but is still poorly understood [8, 9, 10, 11, 12, 13, 14].

Another field of fundamental interest in ferroelectrics is to influence dipole behaviors by, e.g., applying electric fields [15, 16] or pressure[17, 18]. The interest stems from the fact that external stimuli often alter the balance among different interactions inside FEs [19], thereby giving rise to new phenomena. In this context, curled electric field (namely, the electric field generated not by static charges, but by time-dependent magnetic field via $\nabla \times \mathbf{E}_{\text{curl}} = -\partial\mathbf{B}/\partial t$) is an interesting route for modifying the behaviors of dipoles since the field possesses non-vanishing curl. The \mathbf{E}_{curl} fields can be generated on FE particles using focused laser beams and by varying the \mathbf{B} -field component of the laser. But effects of curled fields in FE nanoparticles have never been studied before (to our knowledge). The knowledge as to how the interaction between FE dipoles and curled electric fields changes the phase properties remains entirely unknown. Technology wise, understanding the response of FE vortex to curled electric fields is of immense relevance, since use of bistable vortex states promises to increase the density of nonvolatile ferroelectric random access memories by five orders of magnitude.[6] Reversing the toroid moment, by applying curled electric fields, is a key process for making this possible. Recently, a study of using *static* electric fields to influence the formation of vortex in FE particles was reported[20], where the system is first heated to high temperatures so that the original vortex disappears, and then the paraelectric particle is annealed under the influence of external static fields. By adopting different external fields, vortices of varied orientations were obtained after annealing. Obviously this is not a switching process in which a constant temperature is maintained.

Independent of both subjects given above, a third topic of importance is to understand switching mechanism in FEs. In *bulk* FEs, coexistence of $-\mathbf{P}$ and \mathbf{P} domains has been widely accepted as the mechanism for polarization switching.[15] More specifically, the switching begins by nucleation of a $-\mathbf{P}$ domain of reversed polarization; crystal defects (domain walls,

twin boundaries, etc.) often are the nucleation sites.[21] Subsequently, the $-\mathbf{P}$ domain grows while the original \mathbf{P} domain shrinks under external fields, leading eventually to switching. In FE nanoparticles, formation of domain walls is less likely and energetically unfavorable. However, the vortex phase in FE particles does have an intrinsic topological defect—the vortex core. Based on the fact that a large strain energy exists near the center of the vortex where dipoles turn their directions sharply, vortex cores are thus less stable. When imposed under a switching curled field, dipoles near the vortex core are likely to flip first to form a $-\mathbf{G}$ domain of reversed moment. This $-\mathbf{G}$ domain coexists with and gradually conquers the \mathbf{G} domain, leading to switching.

Here we perform *ab initio* based studies to investigate for the first time the collective response to curled electric fields, and the vortex switching mechanism, in ferroelectric nanoparticles made of $\text{Pb}(\text{Zr}_{0.5}\text{Ti}_{0.5})\text{O}_3$ solid solution. The purpose of this Letter is (1) to demonstrate that the generally accepted mechanism of domain coexistence is invalid for vortex switching, and in fact, vortex reversal occurs by following an interesting G_z - G_y - $(-G_z)$ phase transformation sequence; (2) to report the unusual collective phenomena and energetics in 0D FEs in response to curled electric fields. Based on the key insight obtained in this study, we further propose and demonstrate an alternative approach (which could be technologically very important) to overcome the energy barrier of vortex switching. It should be pointed out that this work is profoundly different from a previous study[22] where effects of *homogeneous* electric fields in FE particles were investigated. Homogeneous electric fields, possessing no curl, can only transform a vortex phase into a ferroelectric phase of polarization. As a result, the switching of toroid moment, which is the key subject of this study, was not (and can not even be) addressed in Ref.22.

Technically, we use first-principle derived effective Hamiltonian[23, 24] and finite temperature Monte Carlo (MC) simulations. Besides internal energy U , the Hamiltonian also consists of a $-\sum_i \mathbf{E}(\mathbf{r}_i) \cdot \mathbf{p}_i$ term,[16] describing the coupling between external electric field $\mathbf{E}(\mathbf{r})$ and local dipoles \mathbf{p}_i . Nanoparticles of disk shape are considered, with cylindrical z -axis parallel to the crystallographic [001] direction. Switching simulations under curled electric fields are performed at 64K where the vortex phase is stable. A fixed acceptance rate of 0.25 and 10000 MC sweeps are used throughout all simulations.[25] We will mainly present results for a disk with diameter $d=19$ and height $h=14$ (both quantities are measured in lattice constant $a=4\text{\AA}$ of pseudocubic bulk), since the diameter (7.6nm) of this disk falls into the

size range (5-50nm) of experimentally fabricated nanoparticles[26]. In this work we use MC rather than molecular dynamics (MD) to study switching dynamics, based on the following considerations. (i) In both methods the basic quantity governing the dynamics is the same, which is the energy. The difference is that the energy is reflected in MD by using forces, while in MC the energy itself is used in determination of next configuration. (ii) Monte Carlo step can be quantified as a “quantum” time, and the equivalence of two methods was rigorously demonstrated in Ref.27, where Monte Carlo simulations and Langevin dynamics yield excellent agreement. (iii) Vortex reversal in FE particles is essentially a thermally activated process (which is slow). MD simulations will be time consuming. But computations of MC simulations are moderate. The method in Ref.23 is extended here to include both static homogeneous \mathbf{E}_h electric field and curled \mathbf{E}_{curl} field, i.e., $\mathbf{E}(\mathbf{r}) = \mathbf{E}_h + \mathbf{E}_{\text{curl}}(\mathbf{r})$. The latter is given as $\mathbf{E}_{\text{curl}} = \frac{1}{2} \mathbf{S} \times \mathbf{r}$, where $\mathbf{S} = S\mathbf{e}_z$ measures the vorticity of the field. With the \mathbf{E}_h and \mathbf{E}_{curl} fields acting together, the interaction energy $-\sum_i \mathbf{E}(\mathbf{r}_i) \cdot \mathbf{p}_i$ becomes $-N(\mathbf{E}_h \cdot \langle \mathbf{p} \rangle + \mathbf{S} \cdot \mathbf{G})$, where N is the number of 5-atom cells in nanoparticles, $\langle \mathbf{p} \rangle$ the average dipole moment, $\mathbf{G} = \frac{1}{2N} \sum_i \mathbf{r}_i \times \mathbf{p}_i$ the toroid moment. Vector \mathbf{S} thus is the thermodynamically conjugated field for toroid moment \mathbf{G} .

Figure 1a depicts the collective behaviors of the toroid moment \mathbf{G} , evolving during simulation as a function of MC sweeps (denoted as n , in units of 200), in the d=19 disk under a curled field of $S=0.25 \text{ mV}/\text{\AA}^2$ that has an opposite vorticity with respect to the initial FE vortex. One key finding in Fig.1a is that the vortex reversal process is predicted to consist of three evolution phases in which the system displays distinct dipole behaviors. These phases are, when MC sweep n is below $n_1=30$ (to be named as phase I), n is between $n_1=30$ and $n_2=43$ (to be referred to as phase II), and $n > n_2$ (phase III). At the initial instant of the simulation, the vortex has only a G_z toroid moment, while the G_x and G_y components are null. As the curled field is turned on, most notable results occurring in Fig.1a are: (1) The G_z moment remains remarkably stable and subjects to only marginal decrease throughout phase I. However, the system does not idly wait; another critical activity is taking place in phase I. That is, the FE nanoparticle is building its G_y moment which increases appreciably and becomes very significant (with a value of $15 \text{ e}\text{\AA}^2$) in the end of phase I. (2) As the system enters phase II, dramatic difference occurs. The G_z moment starts to decline sharply, reverses its direction, and then is stabilized at its negative saturated value at n_2 . (3) While G_z switches its direction in phase II, the G_y moment undergoes a complex evolu-

tion, by first rising (with a different slope than the preceding process in phase I) and later dropping swiftly to null. Precisely at the moment when G_z is zero, G_y reaches its maximum magnitude.

From simulations, the key toroid component during switching is G_z , G_y and $-G_z$ for the phases of $n < n_1$, $n_1 < n < n_2$, and $n > n_2$, respectively. The reverse of FE vortex therefore occurs by undergoing an evolution sequence of $G_z \rightarrow G_y \rightarrow (-G_z)$, in which appearance of the lateral G_y moment is a critical bridging process. Formation of this lateral vortex is unusual (and puzzling), for neither the initial vortex of the system nor the curl of the external field have nonzero components in the lateral xy directions which are capable of causing the observed collective behaviors. To verify the above switching sequence, calculations with varied initial dipole configurations or temperatures or slightly different \mathbf{E}_{curl} fields were performed. All confirm the occurrence of a lateral vortex as the bridging phase. We also find that the toroid moment of the intermediate lateral vortex can point at any direction within the xy plane, since x - and y -axis are equivalent. In simulations of Fig.1a, the lateral vortex happens to be mainly along the y -axis.

To explain why the G_y toroid moment forms and how it influences the reversal of the G_z component, we now provide *microscopic* insight on the field-induced dipole behaviors. Fig.2 shows the snapshots of local dipole distributions corresponding to selected MC sweeps. More specifically, Fig.2a-d describe the development of the G_y toroid moment, while Fig.2e-h show the evolution of the inplane G_z vortex. Our discussion shall follow the sequential order of evolution. Initial response to the curled electric field is subtle, and begins with the dipoles located at the vortex core. Common wisdom tells us that, under the \mathbf{E}_{curl} field, the dipoles near the vortex core should flip into opposite directions to form a $-\mathbf{G}$ domain. Interestingly, this does not take place in our simulations. We find instead that these dipoles rotate towards the z -axis (Fig.2a). The dipole rotation is, however, energetically less favorable, since it generates a z -direction depolarization field that can not be compensated by the curled field. Note that this situation is unlike the case when a static homogeneous electric field is applied in the z -axis, where the homogeneous field can overcome the existence of the depolarization field. The delicate balance between the internal depolarization field and the external curled field leads to the dipole configuration in Fig.2a, where the dipoles in the lower part point downwards as a result of the curled field while the dipoles in the upper part point horizontally to reduce the depolarization field. As evolution proceeds to $n=20$ (Fig.2b),

dipoles of the lower part rotate also horizontally, but opposite to the dipole direction in the upper part, to avoid lateral depolarizing field. Consequently, the dipole pattern developed in Fig.2b explains how the nucleation seed of lateral G_y vortex is formed (which is important). Another key feature of the dipole pattern in Fig.2b is that the left and right arms of the G_y vortex are largely absent. Interestingly, as the G_y vortex is nucleated at $n=20$, the inplane G_z vortex is nearly intact (see the G_z vortex in Fig.2e, also at $n=20$), which is consistent with the result in Fig.1a where the G_z moment remains robust throughout phase I.

The system behaves differently when evolving into phase II, highlighted in Fig.2f by the dramatic disappearance of inplane dipole components in regions A and B. More precisely, dipoles in region A rotate toward the negative z -axis, while dipoles in region B toward the positive z -direction. Disappearance of the inplane components for dipoles in A and B regions leads to three marked effects: (i) the onset of a sharp decline of the G_z moment, as seen in Fig.1a at the beginning of phase II, (ii) the core of the G_z vortex to shift away from the cylindrical axis (Fig.2f), and (iii) a rapid increase of the z -component magnitudes for those dipoles located at the left and right arms of the lateral G_y vortex, as revealed by contrasting Fig.2c with Fig.2b. It should be recognized that nucleation of the lateral G_y vortex, right in the form of Fig.2b, is critical for the destruction of the original G_z vortex, since the oppositely oriented horizontal dipoles at the upper and bottom surfaces in Fig.2b produce only a small strain energy when the dipoles in regions A and B rotate into the z direction, and simultaneously, no significant increase in the depolarizing field occurs along the z -axis.

As the G_z vortex continues to be uncurled, the G_z moment becomes zero at $n=33$ (see Fig.1a). A vanishing G_z moment does not mean disappearance of the xy components of all dipoles, however. Instead, calculation result in Fig.2g reveals that the dipole components on the xy plane evolve, interestingly, into a stripe pattern, which also yields zero G_z . The stripe is formed due to the fact that the curled field continues to push the G_z -vortex core in Fig.2f to the (lower) surface. Starting with the stripe in Fig.2g, dipoles in the upper part rotate and/or flip their directions, forming the critical embryo of the *reversed* $-G_z$ vortex at $n=34$ (see Fig.2h). After the nucleation of this $-G_z$ vortex, the lateral G_y vortex starts to disassemble itself by rotating its dipoles at both arms back to the xy plane (see Fig.2d at $n=40$), which eventually leads to the development of a full and reversed $-G_z$ vortex.

From the above striking microscopic insight, a novel mechanism that governs the switching of FE vortex is thus obtained. That is, vortex reversal occurs, not by the coexistence of

G_z and $-G_z$ domains, but by formation of a new and lateral vortex. In fact, we find from the entire evolution process in Fig.2 that, the G_z and $-G_z$ domains never coexist at any time in the simulations. Only after the original G_z vortex is dismantled does the nucleation of the $-G_z$ vortex start to form (Fig.2h). We further numerically find that the magnitude of the total toroid moment $|\mathbf{G}| = \sqrt{G_x^2 + G_y^2 + G_z^2}$ is almost a constant throughout the switching (see the diamond symbols in Fig.1a), demonstrating that vortex reversal occurs by obeying the conservation of the $|\mathbf{G}|$ moment.

We now study the energetics of vortex switching. Here we are interested in internal energy U , rather than free energy $F=U-\sum_i \mathbf{E}(\mathbf{r}_i)\cdot\mathbf{p}_i$, since the former yields important knowledge concerning the energy barrier. The internal energy is given in Fig.1a, revealing new observations that do not appear in collective behaviors. First, the highest energy barrier occurs around $n=30$, which corresponds to the instant when the G_y vortex has formed and the inplane G_z vortex just starts to annihilate its xy components. Height of the energy barrier is 2.4 meV per 5-atom cell. Second, and interestingly, a local energy *valley* appears at $n=33$, showing that the fully developed G_y vortex (with $G_z=0$) is actually a stable structure even if the curled field is removed. Third, the two energy barriers surrounding this energy valley are asymmetric, with a lower barrier of 0.8 meV at $n=35$ (favoring the formation of the $-G_z$ vortex). To examine how the energy barrier may vary with temperature and size, we have performed switching calculations at 160K (as compared to 64K in Fig.1a), for the same $d=19$ and $h=14$ dot. The energy barrier is found to be 2.1 meV at 160K, close to the value of 2.4 meV at 64K. This is consistent with the fact that the energy barrier is determined mainly by depolarization field, not by temperature. We have also performed calculations for other d diameters, all showing that formation of the lateral vortex is a key step for switching the G_z vortex. We further find that depending on the h/d ratio, the number of lateral vortices—that occur at the switching moment (i.e., when G_z equals zero)—differs. In the $d=9$ and $h=14$ disk with $h/d \approx 2$, two G_y vortices and one G_x vortex (with dipole configuration similar to the structural B phase in Ref.6) take place at the switching moment. The energy barrier for the $d=9$ disk is found to be 1.7 meV at 64K.

Interestingly, we previously found that *homogeneous* $\mathbf{E}_h = E_h \mathbf{e}_z$ electric fields can also give rise to a lateral vortex[22], despite that homogeneous fields and curled fields are drastically different in nature. Based on the key findings that (1) the \mathbf{E}_h and \mathbf{E}_{curl} fields both are capable of inducing the G_y vortex, and (2) formation of the G_y vortex is the major energy

barrier for toroid switching (as demonstrated in this study), we further propose an alternative approach to switch FE vortex, by means of a combined action of the \mathbf{E}_h and \mathbf{E}_{curl} fields. More precisely, an \mathbf{E}_h field of sufficient magnitude is applied to precipitate the formation of G_y vortex, and an \mathbf{E}_{curl} field is then added on (while the \mathbf{E}_h field remains) to generate the reversed G_z vortex. A significant advantage of this approach is, while a strong curled field is hard to achieve since it requires fast oscillation of alternating magnetic fields, a strong \mathbf{E}_h field of 10^9V/m order can be easily generated on nanometer scale. We demonstrate the approach using the same $d=19$ disk, by placing it first under a homogeneous $E_h=1.9\text{V/nm}$ field (which quickly induces a G_y vortex), and then under a curled $E_{\text{curl}}=0.04\text{mV/\AA}^2$ field for ten thousand MC sweeps. Fig.1b describes the evolution of the toroid moment after the curled field is turned on. Drastic differences are evident in Fig.1b as compared to Fig.1a: (1) When the curled field is switched on, the G_y value in Fig.1b is already notably large. This G_y moment is formed by the homogeneous field, confirming the result of Ref.22. (2) The long period of phase I—that lasts five thousand MC sweeps in Fig.1a—no longer exists in Fig.1b. Instead, G_z starts to decline sharply in Fig.1b as soon as the curled field is imposed. (3) The magnitude of the curled field used in Fig.1b is considerably reduced, by a factor of 600% as compared in Fig.1a. This reduction factor can be further increased when a larger \mathbf{E}_h field is used. Analysis of the internal energy (solid symbols in Fig.1b) shows that the energy barrier almost disappears, and the curled field acts to guide the formation of the reversed vortex.

In summary, response of FE particles to curled electric fields was studied for the first time. Simulations revealed a novel mechanism that governs the switching of FE toroid vortex. A curled electric field, of only z -axis vorticity momentum, was shown to lead to the unexpected formation of a lateral vortex, manifesting *macroscopically* the balance of various *microscopic* interactions. We demonstrated that the strong correlation between the original vortex and the new lateral vortex plays a critical role for vortex reversal. On the other hand, the $-\mathbf{G}$ and \mathbf{G} domains never coexist during switching, and the switching mechanism by coexisting domains is not valid. Moreover, based on the findings that formation of lateral vortex is the major energy barrier for vortex switching, and that this lateral vortex can also occur by use of homogeneous field, we described an effective approach that is able to reduce substantially (by 600%) the magnitude of the switching curled field. Finally, we believe that the microscopic insight and energetics (which are difficult to obtain in experiments) will also

be of immense value.

-
- [1] N. Sai, B. Meyer, and D. Vanderbilt, Phys. Rev. Lett. **84**, 5636 (2000).
 - [2] J.B. Neaton and K.M. Rabe, Appl. Phys. Lett. **82**, 1586 (2003).
 - [3] M.P. Warusawithana *et al.* Phys. Rev. Lett. **90**, 036802 (2003).
 - [4] H.N. Lee *et al.*, Nature **433**, 395 (2005).
 - [5] D.D. Fong *et al.*, Science **304**, 1650 (2004).
 - [6] I.I. Naumov, L. Bellaiche, and H. Fu, Nature **432**, 737 (2004).
 - [7] V.L. Ginzburg *et al.*, Solid State Commun. **50**, 339 (1984).
 - [8] C. Kittel, Phys. Rev. **70**, 965 (1946).
 - [9] N.D. Mermin and H. Wagner, Phys. Rev. Lett. **17**, 1133 (1966).
 - [10] D.J. Thouless, Phys. Rev. **187**, 732 (1969).
 - [11] P.W. Anderson, G. Yuval, and D.R. Hamann, Phys. Rev. B **1**, 4464 (1970).
 - [12] P. Bruno, Phys. Rev. Lett. **87**, 137203 (2001).
 - [13] P. Gambardella *et al.*, Nature **416**, 301 (2002).
 - [14] L.D. Landau and E.M. Lifshitz, *Statistical Physics, Part 1* (Pergamon, NY, 1980).
 - [15] M.E. Lines and A.M. Gluss, *Principles and Application of Ferroelectrics and Related Materials* (Clarendon, Oxford, 1979).
 - [16] A. Garcia and D. Vanderbilt, Appl. Phys. Lett. **72**, 2981 (1998).
 - [17] G.A. Samara, in *Solid State Physics* (ed. H. Ehrenreich and F. Spaepen), Vol. 56, p 240, and references therein.
 - [18] Z. Wu and R.E. Cohen, Phys. Rev. Lett. **95**, 037601 (2005).
 - [19] R.E. Cohen, Nature **358**, 136 (1992); R.E. Cohen and H. Krakauer, Phys. Rev. B **42**, 6416 (1990).
 - [20] S. Prosandeev *et al.*, Phys. Rev. Lett. **96**, 237601 (2006).
 - [21] W.J. Merz, Phys. Rev. **95**, 690 (1954).
 - [22] I. Naumov and H. Fu, Phys. Rev. Lett. **98**, 077603 (2007); cond-mat/0612549.
 - [23] W. Zhong, D. Vanderbilt, and K. M. Rabe, Phys. Rev. Lett. **73**, 1861 (1994).
 - [24] L. Bellaiche, A. Garcia, and D. Vanderbilt, Phys. Rev. Lett. **84**, 5427 (2000).
 - [25] Using the same acceptance rate of 0.25, we find that the bulk polarization in $\text{Pb}(\text{Zr}_{0.5}\text{Ti}_{0.5})\text{O}_3$

is switched within ten thousand MC sweeps.

- [26] C. Liu, B. Zou, A.J. Rondinone, and Z.J. Zhang, *J. Am. Chem. Soc.* **123**, 4344 (2001).
- [27] U. Nowak, R.W. Chantrell, and E.C. Kennedy, *Phys. Rev. Lett.* **84**, 163 (2000).

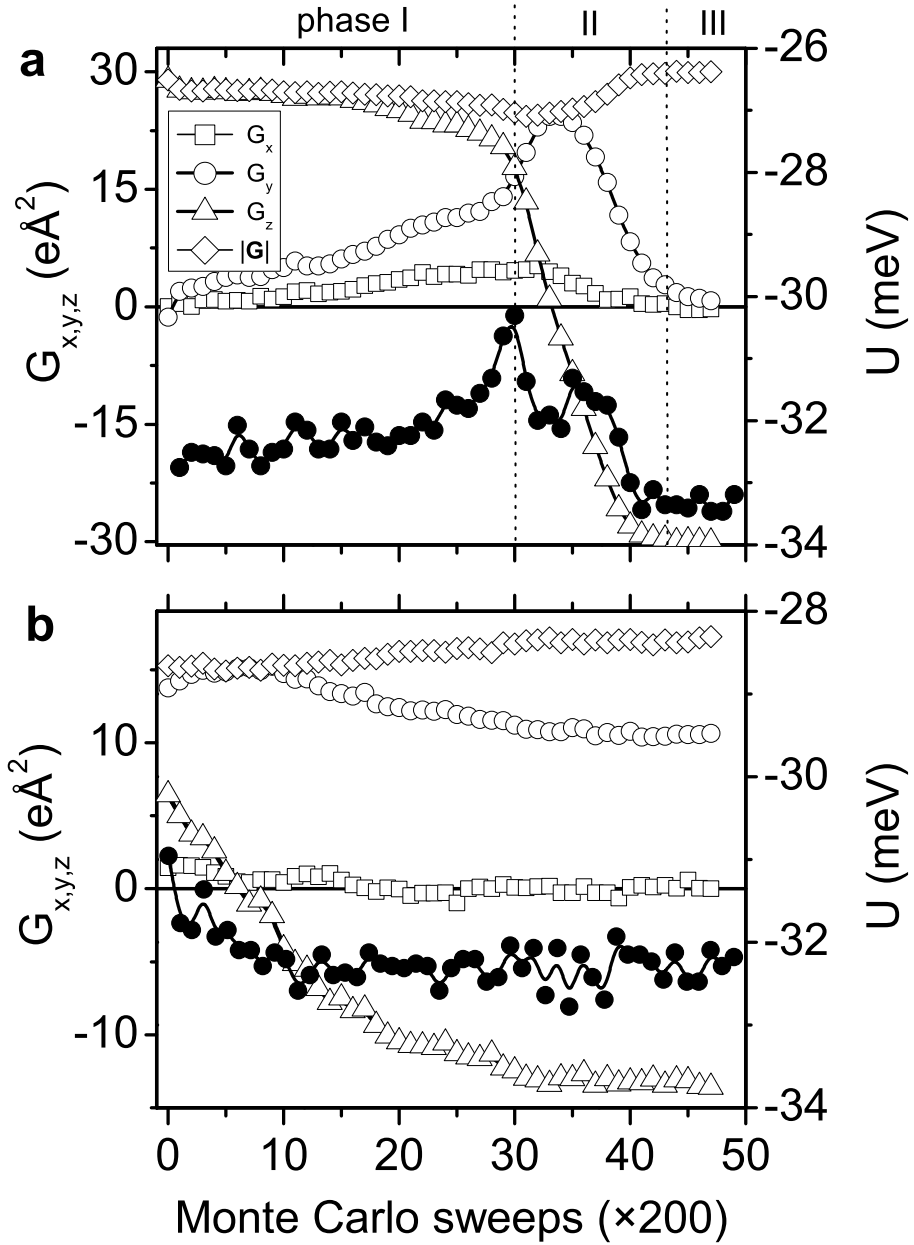


FIG. 1: Evolution of toroid moment \mathbf{G} and its magnitude $|\mathbf{G}|$ (empty symbols, using the left vertical axis) and internal U energy per 5-atom cell (solid dots, using the right vertical axis) in a $d=19$ nanodisk: (a) under a $S=0.25\text{mV}/\text{\AA}^2$ curled electric field; (b) under the combined action of a $E_h=1.9\text{V}/\text{nm}$ homogeneous field and a $S=0.04\text{mV}/\text{\AA}^2$ curled field. For clarity of display, G_z is plotted after multiplying -1 .

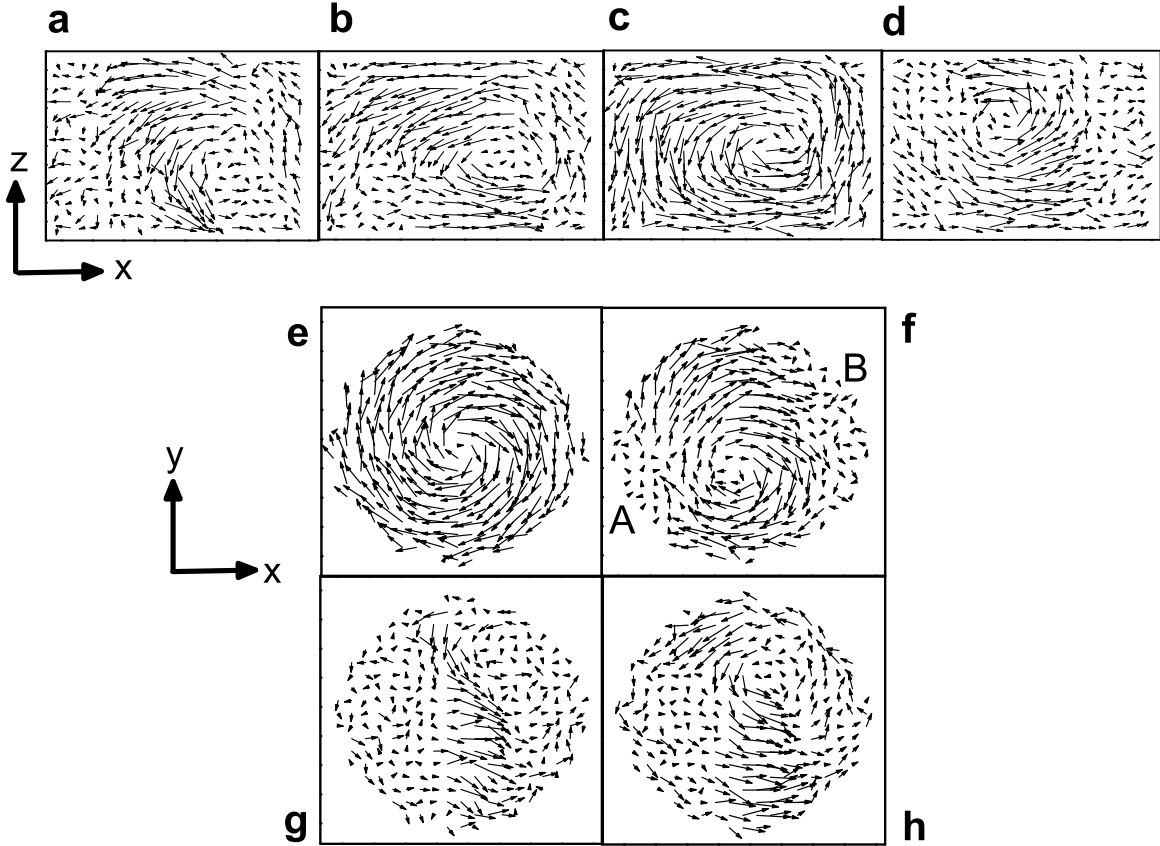


FIG. 2: Dipole configurations in a $d=19$ nanodisk under a curled field of $S=0.25\text{mV}/\text{\AA}^2$ at different MC sweeps. Upper panel (a-d): dipoles on the central xz cross section revealing the evolution of the G_y vortex, at the following MC sweeps (a) $n=10$, (b) $n=20$, (c) $n=30$, (d) $n=40$. Lower panel (e-h): dipoles on the central xy cross section displaying the evolution of the G_z vortex, at (e) $n=20$, (f) $n=30$, (g) $n=33$, (h) $n=34$. All (n) numbers are in units of 200 MC sweeps. Arrows show the magnitudes and directions of local dipoles, projected on the corresponding plane. For convenience, (b) and (e) corresponding to the same $n=20$ sweep are given on the same column [so are (c) and (f)].